Published in final edited form as:
Sci Transl Med. 2013 December 11; 5(215): 215ra172. doi:10.1126/scitranslmed.3006597.

PD-1– and CTLA-4–Based Inhibitory Chimeric Antigen Receptors (iCARs) Divert Off-Target Immunotherapy Responses

Victor D. Fedorov[1,2], **Maria Themeli**[1], and **Michel Sadelain**[1,3,*]

[1]Center for Cell Engineering, Memorial Sloan-Kettering Cancer Center (MSKCC), New York, NY 10065, USA

[2]Tri-Institutional MSTP Program (MSKCC, Rockefeller University, Weill-Cornell Medical College), New York, NY 10065, USA

[3]Molecular Pharmacology and Chemistry Program, MSKCC, New York, NY 10065, USA

Abstract

T cell therapies have demonstrated long-term efficacy and curative potential for the treatment of some cancers. However, their use is limited by damage to bystander tissues, as seen in graft-versus-host disease after donor lymphocyte infusion, or “on-target, off-tumor” toxicities incurred in some engineered T cell therapies. Non-specific immunosuppression and irreversible T cell elimination are currently the only means to control such deleterious responses, but at the cost of abrogating therapeutic benefits or causing secondary complications. On the basis of the physiological paradigm of immune inhibitory receptors, we designed antigen-specific inhibitory chimeric antigen receptors (iCARs) to preemptively constrain T cell responses. We demonstrate that CTLA-4– or PD-1–based iCARs can selectively limit cytokine secretion, cytotoxicity, and proliferation induced through the endogenous T cell receptor or an activating chimeric receptor.

*Corresponding author. m-sadelain@ski.mskcc.org.

Author contributions: V.D.F. conceived the iCAR design, planned and performed the experiments, and wrote the manuscript. M.T. helped in performing experiments, provided intellectual input, and edited the manuscript. M.S. directed the study, planned the experiments, and wrote the manuscript.

Competing interests: The authors declare that they have no competing interests. V.D.F. and M.S. have filed a patent pertaining to the results presented in the paper [title: Compositions and methods for immunotherapy, attorney docket number: 92622P(51590)].

SUPPLEMENTARY MATERIALS
www.sciencetranslationalmedicine.org/cgi/content/full/5/215/215ra172/DC1
Fig. S1. CTLA-4 iCAR cell surface expression is increased after T cell activation.
Fig. S2. iCAR-P bind to PSMA-expressing cells.
Fig. S3. Allogeneic reactivity model using iPS-derived fibroblasts and isogenic moDCs.
Fig. S4. Potent reactivity of iCAR-transduced primary human T cells against allogeneic iPS-derived fibroblasts.
Fig. S5. Transduction and sorting strategy of iCAR or 19-28z/iCAR T cells.
Fig. S6. Sorting strategy of low/high iCAR–expressing T cells and PSMA-expressing iPS fibroblasts.
Fig. S7. iCARs inhibit 19-28z–driven human T cell cytokine release and proliferation.
Fig. S8. Basal expression of iCARs does not affect function of primary human T cells.
Fig. S9. Signaling and biochemical pathway characterization of the PD-1 iCAR.
Movie S1. iCAR- and CAR-expressing T cells discern targets in vitro.
Table S1. Raw data and statistical significance testing for Fig. 2.
Table S2. Raw data and statistical significance testing for Fig. 3.
Table S3. Raw data and statistical significance testing for Fig. 4.
Table S4. Raw data and statistical significance testing for Fig. 5.

The initial effect of the iCAR is temporary, thus enabling T cells to function upon a subsequent encounter with the antigen recognized by their activating receptor. iCARs thus provide a dynamic, self-regulating safety switch to prevent, rather than treat, the consequences of inadequate T cell specificity.

INTRODUCTION

T cell therapies have shown clinical efficacy in bone marrow and organ transplantation, cancer immunotherapy, viral infections, and auto-immune diseases (1–6). Unfortunately, T cells may also engage in deleterious side effects. “On-target but off-tumor” adverse events have been reported in cancer immunotherapy clinical trials using both T cell receptor (TCR)– and chimeric antigen receptor (CAR)–engineered T cells. These include B cell aplasia in chronic lymphocytic leukemia patients treated with T cells expressing anti-CD19 CAR (7–9), fatal acute respiratory distress syndrome after anti-ERBB2 CAR T cell infusion thought to result from cross-reactivity on lung epithelium (10), and TCR-induced fatalities from cardiac myonecrosis or neurological toxicity incurred in patients treated with TCRs recognizing cancer-testis antigens (11–13). Similarly, the curative gains of donor lymphocyte infusion (DLI) in allogeneic bone marrow transplantation are hampered by the induction of both acute and chronic graft-versus-host disease (GVHD) and bone marrow aplasia (14). Strategies to separate the beneficial effects of graft versus tumor (GVT) from GVHD have met with limited success to date (15).

The current approach to curb T cell–mediated toxicities relies on the use of immunosuppressive regimens such as high-dose corticosteroid therapy, which exert cytostatic or cytotoxic effects on T cells, to restrain immune responses (16). Although effective, this approach fails to discriminate between beneficial and deleterious T cell functions. Additionally, immunosuppressive drugs cause substantial secondary side effects, such as susceptibility to infections, and cardiac, kidney, and neurological damage (14). Suicide gene engineering strategies, which may use selective enzymatic metabolizers of toxic agents, such as herpes simplex virus thymidine kinase (17) or inducible caspase-9 (18), or antibody-mediated depletion strategies targeting ectopic epitopes engineered into T cells (19, 20), also eliminate T cells indiscriminately of their therapeutic efficacy. Furthermore, these approaches are reactive because they are implemented after observing deleterious side effects. Strategies that prevent unwanted T cell reactivity are thus highly desirable.

Physiological regulation of T cell activation is accomplished by several mechanisms that include immune inhibitory receptors, which play a pivotal role in attenuating or terminating T cell responses (21, 22). Inhibitory receptors can be up-regulated during T cell priming to taper immune responses or basally expressed to regulate activation thresholds. Thus, mice deficient for the inhibitory receptor CTLA-4 display massive T cell activation and proliferation and eventually succumb to severe systemic autoimmune disease with infiltration of activated T cells (23). Similarly, loss of PD-1, another inhibitory receptor specifically expressed on activated T cells, causes progressive arthritis and glomerulonephritis in C57BL/6 mice and accelerated insulitis in nonobese diabetic (NOD) mice (24, 25). Modulation of these receptors and their downstream signaling pathways has

substantial influence on T cell functions. In vitro ligation of CTLA-4 or PD-1 during T cell stimulation blocks activation, cytokine release, and proliferation (26). Notably, anti–CTLA-4 and anti–PD-1 antibodies have shown clinical promise by derepressing anti–T cell responses in some patients with melanoma, lung, and renal cancer (22, 27, 28). Blockade of both CTLA-4 and PD-1 is also being actively investigated for reversing immune dysfunction and viral persistence in chronic hepatitis B and HIV infection (29, 30). However, similar to nonspecific immunosuppression, antibody-mediated inhibitory receptor checkpoint blockade is not antigen-specific and therefore does not discern between beneficial and deleterious T cell populations.

Here, we used a genetic engineering strategy to harness the natural T cell inhibition physiology and regulate T cell responses in an antigen-selective manner. Conceptually, we sought to design an inhibitory CAR (iCAR) having a surface antigen recognition domain combined with a powerful acute inhibitory signaling domain to limit T cell responsiveness despite concurrent engagement of an activating receptor (Fig. 1A). We show here, in human primary T cells, that PD-1– and CTLA-4–based iCARs reversibly restrict critical TCR or activating CAR functions, and thus allow for discrimination between target and off-target cells in vitro and in vivo.

RESULTS

iCARs are well expressed on the cell surface of primary human T cells

We hypothesized that a single-chain variable fragment (scFv) specific for an antigen fused to the signaling domains of immunoinhibitory receptors (CTLA-4 and PD-1) via a transmembrane region would inhibit T cell function specifically upon antigen recognition. As a first model, we used an scFv specific for human prostate-specific membrane antigen (PSMA) (31). This scFv has been extensively studied and is being investigated in phase 1 trials for immunotherapy of prostate cancer (32). PSMA is overexpressed in metastatic prostate cancer but is also found in normal kidney, liver, colon, and brain astrocytes (33). Along with these two iCARs specific for PSMA (referred to as iCAR-P), we used Pdel, which has the PSMA-specific scFv but lacks a cytoplasmic domain (34), as a control receptor (Fig. 1B). Upon transduction of human primary T cells from peripheral blood mononuclear cells, PD-1–iCAR-P and Pdel were expressed on the cell surface at similar levels to the P28z receptor (34), a CD28/CD3ζ-based, dual-signaling PSMA-specific receptor that is currently used in a clinical trial (Fig. 1C). In the case of the CTLA-4–iCAR-P, we observed robust intracellular expression by Western blot and intracellular flow cytometry, but limited cell surface expression (fig. S1, A and B, and Fig. 1C). This finding is consistent with the physiological trafficking of CTLA-4, which is constitutively internalized in resting T cells and degraded through interaction with the endocytic adaptor complex AP-2 via its tyrosine motif YVKM (35). Indeed, we found up-regulation of the CTLA-4–iCAR-P to the cell surface after T cell activation (fig. S1C), and restored constitutive surface expression using a tyrosine motif Y165G mutant to construct mutCTLA-4–iCAR-P, which exhibited cell surface expression in resting cells (Fig. 1C). PSMA recognition by iCARs was demonstrated using a cellular conjugation assay in which iCAR-expressing T cells bound mouse thymoma EL4 cells expressing PSMA (fig. S2A).

iCARs limit TCR responses in an antigen-restricted manner

To study the effect of iCARs on endogenous TCR-driven primary human T cell responses, we established an alloreactivity model using allogeneic dendritic cells (DCs) as priming antigen-presenting cells and fibroblasts isogenic to the DCs as the targets (fig. S3A). In this model, the iCAR-or Pdel-engineered T cells were primed with allogeneic monocyte-derived DCs (moDCs) and then evaluated against fibroblasts expressing the PSMA antigen or not. To obtain replenishable fibroblasts isogenic to the DCs without requiring iterative skin biopsies, we established induced pluripotent stem cells (iPSCs) from which we derived stable fibroblast cell lines, termed iPS-fib (fig. S3, B to D). The iPS-fib displayed replicative senescence and contact inhibition, and could be easily transduced, passaged, and implanted in NOD/severe combined immunodeficient (SCID)/γ_c^- mice wherein they persisted for weeks without forming tumors. To acquire potent alloreactive T cells with endogenous TCR specificity against the iPS-fib, we pulsed moDCs with lysates from the isogenic iPS-fib. This priming culture system stimulated robust cytotoxicity and cytokine secretion from several T cell donors, producing both CD4- and CD8-driven responses (fig. S4, A to C).

To investigate the ability of the iCARs to restrict alloreactivity against PSMA$^+$ cells, we sorted iCAR- or Pdel-expressing T cells primed with two rounds of pulsed moDCs and then co-incubated them with iPS-fib or iPS-fib expressing PSMA (fig. S5A) (36). All groups of T cells efficiently killed iPS-fib, demonstrating allogeneic cytotoxicity (Fig. 2, A and B), but the iCAR-positive T cells were significantly inhibited in their ability to kill iPS-fib-PSMA$^+$ cells (Fig. 2C). Cytotoxicity by T cells expressing the PD-1-based iCAR was reduced by up to 95% at low effector-to-target (E/T) ratios. Because cytotoxicity occurs rapidly and has a low activation threshold relative to other T cell responses, we also analyzed cytokine secretion. The PD-1 iCAR produced the stronger inhibition of cytokine secretion (79 to 88% reduction), whereas the mutCTLA-4 iCAR elicited 55 to 71% reduction (Fig. 2, D to F). These results suggested that iCARs could limit reactivity in an antigen-dependent manner.

iCARs function in a stoichiometric manner

We investigated whether the PD-1 iCAR-P could provide differential levels of inhibition depending on its level of expression or that of the target antigen. We therefore sorted primed T cells for high or low levels of PD-1 iCAR-P or Pdel expression and exposed them to iPS-fib-PSMA (fig. S6A). We found a stoichiometric relationship between T cell killing, cytokine release, and the level of iCAR expressed. T cells sorted for low levels of expression of the PD-1 iCAR-P could provide 50% inhibition only up to E/T ratios of 1:1, but high levels of PD-1 iCAR-P expression allowed 80% inhibition up to E/T ratios of 8:1 and even 50% inhibition at 16:1 (Fig. 3, A and B). To examine the impact of the iCAR antigen expression level, we sorted iPS-fib for high or low PSMA expression and exposed them to sorted PD-1 iCAR-P T cells (fig. S6B). iPS-fib with high PSMA expression inhibited at least 80% of the killing and cytokine secretion of PD-1 iCAR-P T cells across a range of E/T ratios (1:1 to 4:1), whereas iPS-fib with low PSMA expression failed to provide the same level inhibition (Fig. 3, C and D).

iCARs limit allogeneic responses in vivo

To investigate whether an iCAR could protect a tissue from T cell–mediated elimination in vivo, we injected iPS-fib-PSMA$^+$ cells (which also expressed CBL) intraperitoneally into NOD/SCID/γ_c^- mice (fig. S6B). The cells established nodules that could be monitored by bioluminescence imaging (BLI). Five days after injection of 1×10^6 iPS-fib-PSMA$^+$ cells, the mice were treated with 5×10^5 moDC-primed Pdel- or PD-1–iCAR-P–expressing T cells. The Pdel group eliminated the iPS-fib-PSMA$^+$ cells with a significant decrease in the BLI signal (7- to 22-fold), whereas the PD-1–iCAR-P group was unable to clear the nodules with BLI similar to control mice not treated with T cells (Fig. 4, A and B). These results provide evidence that an iCAR can limit a TCR-driven response in an antigen-specific fashion in vivo.

iCARs can inhibit activating chimeric antigen receptors

To study the effect of iCARs on modulating activating CARs, we used 19-28z, an extensively characterized second-generation CAR currently used in clinical trials, which provides activation and CD28 costimulation in response to the CD19 antigen (9, 34). Primary T cells were transduced with 19-28z CAR and the iCAR-P receptors, sorted for dual expression, and seeded on previously reported artificial antigen-presenting cells (AAPCs) expressing CD19 or both CD19 and PSMA, respectively, modeling target and off-target tissues (37) (figs. S5B and S7A). Although the T cells from the control groups (19-28z alone or 19-28z/Pdel) showed similar cytokine secretion on both AAPCs, the iCAR-expressing T cells showed a marked decrease in cytokine secretion when exposed to off-target cells relative to on-target cells (Fig. 5A and fig. S7B). PD-1 iCAR-P produced the strongest reduction of cytokine levels (71 to 89%), whereas mutCTLA-4 iCAR-P elicited a lesser reduction (48 to 67%).

19-28z provides a potent proliferation signal, induced by CD19-expressing AAPCs. Although 19-28z/Pdel T cells expanded similarly on either AAPCs, T cells expressing mutCTLA-4 or PD-1 iCARs showed reduced accumulation in the presence of the off-target AAPCs, with the PD-1 iCAR-P causing a cumulative 90% decrease in T cell accumulation after the second AAPC stimulation (Fig. 5, B and C, and fig. S7C). In this coculture system, we examined by quantitative microscopy the fate of these AAPCs, which we modified to additionally express mCherry (Fig. 5D). Within 38 hours, all groups of 19-28z/iCAR-P and control double-positive T cells lysed the target cells (Fig. 5E). When exposed to CD19$^+$PSMA$^+$ off-target cells, the mutCTLA-4– and PD-1–based iCARs caused a 67 and 91% reduction in cytotoxicity, respectively (Fig. 5F). In the case of PD-1, AAPCs persisted for 5 days, whereas the effect of the mutCTLA-4 iCAR was more limited (Fig. 5D). We therefore selected the PD-1–based iCAR for further in vivo evaluation.

To evaluate the function of the PD-1 iCAR in vivo, we transduced NALM/6, a CD19$^+$ B cell leukemia cell line, with PSMA, and compared therapeutic T cell responses against NALM/6 and NALM/ 6-PSMA cells in a previously established xenograft NOD/SCID/γ_c^- mouse model (37, 38) (fig. S7D). Five days after systemic tumor infusion, the mice were treated with a single dose of 3×10^5 19-28z/PD-1–iCAR-P–sorted double-positive T cells. BLI of tumor burden showed significant differences (3- to 10-fold reduction) in the eradication of

NALM/6-PSMA (off-target) as opposed to NALM/6 (on-target) (Fig. 6, A and B). Although initially confined to bone marrow, NALM/6 leukemia eventually invades the spleen, the weight of which provides a late-stage index of disease burden. After treatment with 19-28z/PD-1–iCAR-P T cells, NALM/6-PSMA mice showed no significant difference in spleen weight from the control "no T cell" group, but the spleen weights of the mice with NALM/6 were 2.6-fold lower (Fig. 6C). Flow cytometric analyses confirmed the decreased number of NALM/6 cells in the spleen and bone marrow, in contrast to the NALM/6-PSMA group (Fig. 6, D and E). In parallel, we found greater persistence of T cells in the NALM/6 group than in the NALM/6-PSMA group (Fig. 6, D and F). These findings established that the PD-1–based iCAR selectively prevents the elimination of "off-target" NALM/6-PSMA cells in vivo while allowing the therapeutic response against "on-target" NALM/6 cells to proceed.

iCARs function in a temporary and reversible manner

An attractive aspect for the clinical usefulness of iCARs is functional reversibility, that is, the reemergence of T cell functionality after previous contact with an inhibitory off-target tissue. Constitutive expression of the iCARs did not impair the T cells' proliferative capacity (post-CD3/CD28 bead or DC activation), cytokine secretion, or surface marker expression compared to control T cells (fig. S8, A to E). To assess the temporal features of iCAR-medicated inhibition, we set up sequential T cell stimulation by target and off-target cells, analyzing the potential for killing, cytokine secretion, and proliferation in four different sequences. 19-28z/Pdel or 19-28z/PD-1–iCAR-P T cells were exposed to either the target ($CD19^+$) or off-target ($CD19^+PSMA^+$) AAPCs as a first stimulation, followed by exposure to either AAPCs in a second stimulation (Fig. 7A). On the second stimulation, both T cell groups killed target cells equally well irrespective of the first stimulation target (Fig. 7B), supporting that the 19-28z/iCAR-P T cells exposed to off-target cells in the first stimulation killed target cells and proliferated during the second stimulation as well as the T cells that were exposed to target cells in both stimulations. Control T cells expressing the 19-28z/Pdel did not show reduced functionality under the same conditions. Additionally, T cells that were activated on the first stimulation could still be inhibited upon exposure to the iCAR ligand presented by the off-target AAPCs on the second stimulation, suggesting that iCARs could regulate an activated T cell. We also observed that T cells exposed to off-target cells on both stimulations had greater inhibition of their killing capacity on the second exposure (Fig. 7, C and D).

Corroborating these functional findings, we found that the PD-1 iCAR, 19-28z/Pdel, and 19-28z/PD-1–iCAR-P double-positive T cells differentially phosphorylated the regulatory SHP-1 and SHP-2 phosphatases (fig. S9). Exposure to $CD19^+$ target AAPCs showed lower SHP-1 and SHP-2 phosphorylation levels compared to the basal levels seen after exposure to AAPCs lacking CD19, consistent with previous studies demonstrating dephosphorylation and consequent blockade of the suppressive effects of SHP-1/2 upon T cell activation (39, 40). In contrast, after exposure to off-target AAPCs expressing CD19 and PSMA, SHP-1 and SHP-2 showed increased levels of phosphorylation, supporting that the PD-1 iCAR recruits the same biochemical pathways as the endogenous PD-1 molecule.

iCAR and CAR dual-expressing T cells discern targets in vitro and in vivo

Finally, we sought to assess whether T cells expressing the PD-1–based iCAR could distinguish between target cells in vitro and especially in vivo by protecting off-target cells in the presence of target cells within the same organism. We first addressed this scenario in an in vitro coculture system mixing GFP^+CD19^+ target AAPCs and $mCherry^+CD19^+PSMA^+$ off-target AAPCs at a 1:1 ratio. We performed time-lapse microscopy to analyze the effect of 19-28z/Pdel or 19-28z/iCAR-P T cells. Both the target and the off-target cells were eliminated at a similar rate by 19-28z/Pdel T cells, but the 19-28z/iCAR-P T cells preferentially eliminated the target cells while sparing the off-target cells (Fig. 8A and movie S1, A and B). Crisscross experiments with CBL-transduced versions of the AAPCs were used to quantify this selectivity. At 38 hours, the 19-28z/iCAR-P T cells eliminated most (85%) of the target AAPCs but few (10%) of the off-target cells, corroborating the results from the time-lapse microscopy (Fig. 8B).

To analyze whether the same selectivity could be attained in vivo, we injected NOD/SCID/γ_c^- mice with a mixture of NALM/6 and NALM/6-PSMA tumor cells and treated these animals with 19-28z–or 19-28z/iCAR-P–transduced T cells. Upon sacrifice, the mice treated with 19-28z T cells showed a threefold reduction in the number of $PSMA^+$ cells in the spleen and bone marrow compared to mice treated with 19-28z/iCAR-P T cells (Fig. 8, C and D). Accordingly, the iCAR-treated group had a 3.3-fold increase in spleen weight and overall increased tumor burden (Fig. 8E). These experiments demonstrate that, in the presence of a mixture of target and off-target cells, an iCAR can selectively protect off-target cells without abrogating rejection of target cells.

DISCUSSION

Here, we take a genetic approach to restrict the specificity of T cells and demonstrate that T cells can be engineered to have an endogenous regulatory targeting mechanism to deliver tumor-specific immunotherapy. We successfully combined an antigen recognition domain with the signaling domains of immune inhibitory receptors CTLA-4 and PD-1 to achieve antigen-specific suppression of T cell cytotoxicity, cytokine release, and proliferation. This proof-of-concept study demonstrates the potential for iCARs as a strategy to limit T cell function at off-target sites and thus divert immune responses away from unintended target tissues.

The crux of the iCAR strategy relies on three critical properties. The first is that basal expression of the iCAR does not inhibit T cell function in the absence of antigen. Endogenous CTLA-4 or PD-1 signaling requires the presence of the respective ligands to exert their effect. Likewise, we did not find expression of the iCARs described herein to affect basal T cell functions. Other inhibitory receptors that are restricted to T cell subsets may act in concert to fine-tune the regulation of T cell responses (21, 22). Receptors such as LAG-3, 2B4, and BTLA and their combination (for example, as a single second-generation iCAR with multiple combined cytoplasmic domains) warrant further investigation.

The second key property is the maintenance of T cell functionality despite previous engagement of the iCAR. We found that iCAR-transduced T cells could still mount a

response against a target antigen after a previous exposure to an inhibitory antigen. This reversibility is reminiscent of natural killer cell behavior, in which the phosphorylation state of signaling molecules rather than transcriptional changes control rapid functional responses, such as cytotoxicity (41). Anti–PD-1 and anti–CTLA-4 antibodies are able to reverse the impaired function of anergized or exhausted T cells, again arguing for the ability to temporally regulate T cell responses (22). Additionally, biochemical analyses of PD-1 and CTLA-4 effects on the TCR complex depend on phosphorylation states, downstream kinases, and motility rather than apoptosis (40, 42–44). Although both our in vitro and in vivo results demonstrate inhibition in response to off-target cells with sustained therapeutic functionality, there is still the possibility that some of the cells may be anergized over time (42). Ultimately, a T cell infusion is stochastic, with some T cells promptly encountering their target and eliminating it, whereas other T cells will first encounter the inhibitory cells. It is conceivable that T cells that repeatedly encounter off-target cells will not expand—a satisfactory outcome for the iCAR strategy, which aims to allow for therapeutic responses to proceed while diminishing the immune attack against normal tissues. The overall expansion of the infused T cell population will integrate these different paths occurring at the clonal level, with some T cells undergoing expansion while others are suppressed, possibly resulting in the disappearance of all infused T cells over time. Under our experimental conditions, enough T cells persisted over 3 weeks to eliminate the targeted tumor. Under such a circumstance, a second or third T cell infusion could be infused if needed, which may be clinically advantageous as discussed elsewhere (9). The eventual induction of anergy and clonal elimination as a means to protect off-target tissues while allowing tumor elimination to proceed should be contrasted to suicide gene strategies where adverse reactivity must manifest itself before T cell elimination is triggered, which results in terminating therapeutic responses as well.

Third, the iCAR approach is antigen-specific and thus requires the ability to identify tissue-specific target antigens that are absent or down-regulated on the tumor but expressed by the off-target tissues. This question has not been as broadly investigated as the search for tumor antigens, although efforts, such as the Protein Atlas database, are under way to characterize the “surfaceome” of all human tissues (45). One strategy is to use broad classes of surface antigens that are down-regulated on tumor cells. One example is represented by human leukocyte antigen (HLA) molecules, which are found in virtually all cell types, but are down-regulated on tumors as a mechanism of tumor escape from T cell immune responses (46). Thus, allogeneic T cells expressing an iCAR against a host HLA molecule that is down-regulated on the tumor may selectively promote the GVT effect. The iCAR approach may be of particular interest in the setting of DLI as a means to protect GVHD target tissues without impairing GVT responses. Another class of antigens amiable to a similar strategy includes cell surface tumor suppressor antigens, such as OPCML, HYAL2, DCC, and SMAR1 (47–49). OPCML-v1, for example, is widely expressed in all normal adult and fetal tissues but is down-regulated in lymphomas and breast and prostate cancer. Cell surface carbohydrates, lipids, and posttranslational modifications, such as mucin-type *O*-glycans (core 3 *O*-glycans) have also been found to be down-regulated by tumors (50). Another candidate target is E-cadherin, which is highly expressed in normal skin, liver, and gut—the

primary targets of GVHD (51)—but down-regulated by tumor cells undergoing an epithelial to mesenchymal transition, indicating tumor progression and metastasis (52).

A major limitation of our study is the lack of availability of a robust clinically relevant human “normal tissue” model, especially one that allows utilization of human cells, human antigens, and human TCRs, CARs, and iCARs. We attempted to bridge this gap by establishing iPS cells combined with DCs from the same donor to derive an alloreactivity reaction using human T cells, human target antigens, and human iCARs. Simply co-incubating HLA mismatched allogeneic T cells with iPS or iPS-fib cells did not produce alloreactivity. The use of isogenic DCs was critical to generating potent alloreactivity. However, we did not define the nature of this alloreactivity, and it is thus possible that the responses we blocked have no bearing on the mechanisms involved in GVHD.

We also showed that the level of expression of the iCARs is critical. In settings of high expression level of activating receptor or antigen and/or low expression of iCAR or iCAR-targeted antigen, we could not achieve sufficient blockade. In most of our analyses, the iCAR reduced T cell function but did not abrogate it, rarely exceeding 90% inhibition in any assay. In applying the iCAR strategy in a clinical setting, the functionality of every iCAR will need to be optimized on the basis of receptor affinity, receptor expression level (that is, promoter strength), and selection of suitable target antigens based, in part, on their expression level. These will also need to be balanced against the activating receptor to achieve inhibition at off-target sites. In the case of CAR-targeted therapy, an optimized CAR/ iCAR ratio could be achieved through careful vector design.

In conclusion, we provide a proof of concept that antigen-specific inhibitory receptors can successfully redirect T cell proliferation, cytokine secretion, and cytotoxicity upon engagement of specific cell surface antigens, thus diverting T cell toxicity away from one tissue while retaining critical effector function against another expressing the same antigen. We showed this in responses mediated by either TCRs or CARs. This approach prevents, or at least reduces, damage to unintended target tissues and thus obviates the need to irreversibly eliminate therapeutic T cells after unacceptable toxicity has developed. It is a paradigm-shifting approach that takes advantage of the multifaceted functionality of cells as drugs by using synthetic receptors that guide and educate T cells to only perform beneficial functions. This dynamic safety switch may find useful applications in a range of autologous and allogeneic T cell therapies.

MATERIALS AND METHODS

Study design

The purpose of this study was to create a synthetic receptor that could limit T cell toxicity toward a target cell in an antigen-dependent and reversible manner. We designed two such receptors using intracellular tails of CTLA-4 or PD-1 and an scFv targeting domain (against PSMA) and analyzed whether they could block (i) TCR- or (ii) CAR-driven T cell functionality in vitro and in vivo. In vitro, the focus was on analyzing (i) cytotoxicity, (ii) cytokine secretion, and (iii) T cell proliferation. In vivo experiments analyzed the integrated ability of the iCAR to protect a cellular target using live imaging and endpoint analysis

(dictated by the untreated group of mice). The experimental procedures were approved by the Institutional Animal Care and Use Committee of Memorial Sloan-Kettering Cancer Center (MSKCC). The general design of the experiments was to expose T cells (expressing iCARs or the control Pdel receptor) to target cells (that expressed or lacked PSMA) and compare the groups trying to interrogate iCAR function, always in the presence of internal controls. We limited T cells lacking iCARs from contaminating the results by sorting T cells to be iCAR or iCAR/CAR double-positive (using reporter genes). Each experiment was performed multiple times using different donor T cells (T cells were never pooled). In most cases, we present data using a representative experiment (with sample replicates of more than three) to avoid confounding variables such as differences due to transduction and sorting efficiencies, donor-related variability, and E/T ratios.

iCAR construction

Each iCAR receptor was designed with the UniProt sequence annotation using two approaches. First, using commercial gene synthesis or cDNAs, the intracellular domain of each receptor was cloned in place of the CD28/CD3ζ domain of the previously described Pz1 receptor (53), thus using the CD8 transmembrane and hinge domains. Alternatively, we included the transmembrane domains and the amino acids up to the first annotated extracellular topological domain (for PD-1, amino acids 145 to 288; for CTLA-4, amino acids 161 to 223) so as to use the endogenous hinge region of each receptor. These constructs were cloned into the P28z vector after the PSMA scFv. We did not find significant functional differences between the receptors generated by the two approaches. We additionally created versions of each iCAR that lacked any targeting domain, but retained the transmembrane and intracellular portions of each receptor. The control Pdel receptor was designed by excising the CD28/CD3ζ domain of P-28z (34). iCARs should be clearly distinguished from CARs, all of which trigger T cell activation, in stark contrast to iCARs.

Conjugation assay, Western blots, and GAM staining

Cell surface expression of each iCAR was analyzed using the previously described goat anti-mouse staining protocol (38). Cellular conjugation assay was performed as previously described (54). Briefly, EL4 or EL4-PSMA cells were labeled with the lipophilic DiD dye (Invitrogen) and mixed at a 1:1 ratio with T cells in fluorescence-activated cell sorting (FACS) tubes, incubated at 37°C for 5 min, and analyzed on a flow cytometer. Western blot analysis was performed using standard protocols with a Bio-Rad Mini-PROTEAN Tetra system. Intracellular tail of CTLA-4 was detected using the polyclonal antibody C-19, which recognizes the CTLA-4 C terminus (Santa Cruz Biotechnology).

Retroviral vectors and viral production

Plasmids encoding the SFG retroviral vector were prepared using standard molecular biology techniques. Synthesis of 19-28z–IRES–LNGFR, CD19, PSMA, GFP, mCherry, and CBL vectors has been described (37, 38, 53). Retroviral producers were prepared from plasmid-transfected H29 cell supernatant as previously described (53).

Cell lines

EL4-CD19, EL4-PSMA, and the AAPCs NIH3T3-CD19 and NIH3T3-PSMA have been described (31, 34, 37, 38, 53). NIH3T3-CD19-PSMA, NIH3T3-CD19-mCherry, NIH3T3-CD19-GFP, and NIH3T3-CD19-CBL, as well as NALM/6-CBL and NALM/6-PSMA-CBL, were obtained after transduction with respective retroviral supernatants of H29 producer cells. All comparative groups of cell lines were sorted for equivalent expression of CD19, GFP, or mCherry with a MoFlo sorter.

Peripheral blood leukocyte collection and retroviral transduction

Peripheral blood was obtained from healthy donors after informed consent under a protocol approved by the MSKCC institutional review board. Peripheral blood leukocytes were isolated with Ficoll-Paque and activated with phytohemagglutinin (PHA) for 48 hours. Activated T cells were transduced on three consecutive days by centrifugation in retronectin-coated (Takara), retroviral vector–bound plates. Cells were fed every 3 days with RPMI medium supplemented with 20 U of interleukin-2 (IL-2). Ten days after transduction, FACS selection based on enhanced GFP (marking the iCARs) and LNGFR (marking 19-28z) was used to isolate positive cells on a MoFlo sorter. Post-sort analysis was performed to ensure equivalent expression of both reporters.

Generation of iPS-derived fibroblasts

Peripheral blood lymphocytes were activated with PHA, transduced with retroviral supernatants (f-citrine-P2A-Myc-E2A-Sox2 and f-vexGFP-P2A-Okt4-T2A-Klf4), and plated after 24 hours on mouse embryonic fibroblast feeder cells (55). Medium was changed to human ES medium with fibroblast growth factor (8 ng/ml) at day 5 after transduction, and half-medium change was performed daily after that. T-iPS colonies appeared at about 22 to 25 days after transduction. A subcutaneous xenograft teratoma assay was performed with the T-iPS-1.10 cell line. At 3 months, the teratoma was removed and treated with collagenase (100 U/ml) (Invitrogen) and dispase (2 U/ml) (Invitrogen) for 2 hours at 37°C to generate a single-cell suspension. The cells were sorted for HLA-ABC–positive cells, and after 1 week in culture in RPMI supplemented with 1% L-glutamine, 1% penicillin, 1% streptomycin, and 10% fetal bovine serum (FBS), they reproducibly spontaneously generated the iPS-fib.

Flow cytometry

All flow cytometric analysis was done on an LSRII cytometer (BD Biosciences) and analyzed with FlowJo software version 9.6 (Tree Star). Anti-human LNGFR, CD45, CD140b, CD10, HLA-ABC, HLA-DR, CD80, CD86, and CD62L were obtained from BD Biosciences; anti-human CD4, CD8, CD3, CD19, CD90, and 4′,6-diamidino-2-phenylindole (DAPI) were obtained from Invitrogen; anti-human PSMA was obtained from Medical & Biological Laboratories; anti-human CCR7 was obtained from R&D Systems; and anti-human Foxp3 (236A/E7) and Foxp3 isotype were obtained from eBioscience.

In vitro T cell assays

In general, for proliferation, effector cytokine production assays, and cytotoxicity assays, serial dilutions of sort-purified T cells were seeded on respective AAPCs (irradiated with 40

to 50 Gy and seeded 24 hours earlier at 3×10^4 per well) in 96-well flat-bottomed plates. iPS-fib were not irradiated when used as targets. Fresh medium was added every 3 to 4 days or upon medium color change. Cytokine production was quantified by either enzyme-linked immunosorbent assay kits (eBioscience) or Luminex assays (Invitrogen) as stated in the text according to the manufacturer's instructions. T cell counts were calculated using viable cell number (DAPI) and CountBright beads (Invitrogen) on an LSR II flow cytometer (BD Biosciences) by collecting whole wells. All in vitro culture experiments were done in RPMI supplemented with 1% L-glutamine, 1% penicillin, 1% streptomycin, and 10% FBS. No exogenous cytokines were administered at any time unless explicitly stated.

Luciferase cytotoxic T lymphocyte assay

Cytotoxic T lymphocyte (CTL) assays using bioluminescence as the readout were performed as previously described (36). Briefly, all in vitro luciferase assays were performed with the Bright-Glo Luciferase Assay System (Promega) and 96-well Optical Bottom Black Microplates (Nunc) and were conducted according to the manufacturer's protocol with minor adjustments. All targets cells were engineered to express CBL with a GFP reporter to ensure equivalent levels of expression. Culture medium was removed to leave 50 μl per well, 50 μl of prepared luciferase reagent was added to each well of the 96-well plates, and the plates were incubated for 5 min to completely lyse the cells. Measurements were performed with the IVIS Imaging System 100 Series (Xenogen). Living Image software version 2.6 (Xenogen) was used to quantify photon emission intensities.

Time-lapse and fluorescence microscopy CTL

All microscopy imaging was performed with a Zeiss AxioVert 200M equipped with a live imaging system. Time-lapse videos were acquired and compiled with Multi Dimensional Acquisition in MetaMorph software (Molecular Devices). For CTL experiments, the signal from mCherry-positive AAPCs was quantitated with the Integrated Morphometric Analysis function in MetaMorph.

moDCs and priming

Monocyte-derived DCs were generated with the Mo-DC Generation Tool Box (Miltenyi) from the same donor as the T-iPS cells. The moDCs were pulsed for 24 hours at the immature stage (days 5 to 6) with lysates from iPS-fib, which were generated through six freeze-thaw cycles. The maturation of the DCs was confirmed by flow cytometry of CD80, CD86, and HLA-DR. Priming was performed as previously described (56). Briefly, the first round of priming was done using a 1:30 T cell/moDC ratio, with the second round using a 1:10 to 1:30 ratio. RPMI supplemented with 1% L-glutamine, 1% penicillin, 1% streptomycin, 10% human AB serum (CellGro), and human IL-15 (5 ng/ml) (R&D Systems) was used. On day 3, IL-2 (20 U/ml) was added.

Proteome profiler array

T cells were exposed to AAPCs at an E/T ratio of 4:1 for 60 min, washed, lysed, and incubated (100 μg) on the Human Phospho-Immunoreceptor Array according to the manufacturer's protocol (R&D Systems). All blots were detected using chemiluminescence

on the same x-ray film to standardize exposure levels. Scanned x-ray film images were analyzed with image analysis software. All pixel density was normalized on each array with internal pY controls.

Mouse models and quantitative bioluminescence

For the NALM/6 studies, 6- to 12-week-old male NOD/SCID/γ_c^- mice (The Jackson Laboratory) were inoculated intravenously with 5×10^5 tumor cells (same dose for either single tumor or mixed tumor experiments). NALM/6 cells were engineered to express CBL with a GFP reporter. Four days later, 3×10^5 sorted T cells were infused intravenously; cell dose was based on the percent $GFP^+19\text{-}28z^+$ as confirmed by post-sort analysis. Mice were sacrificed at 21 days (no T cell controls display hindlimb paralysis). For iPS-fib studies, 6- to 12-week-old male NOD/SCID/γ_c (null) mice were inoculated intraperitoneally with 1×10^6 cells prepared in a 1:1 mixture of ice cold RPMI and Matrigel mixture (BD Biosciences). Eight days later, 5×10^5 twice moDC-primed GFP-sorted T cells were infused intraperitoneally; cell dose was based on the percent GFP^+ as confirmed by post-sort analysis. Additionally, an in vitro luciferase CTL assay was performed to establish equivalent allogeneic reactivity in all groups using iPS-fib as a target. In both models, D-luciferin (Xenogen, 150 mg/kg intraperitoneally) was used as a substrate for click beetle luciferase, and bioluminescence images were collected on an IVIS 100 Imaging System. Living Image software version 2.6 was used to acquire and quantify the BLI data sets as described before (38). Mice were cared for in accordance with the institutional guidelines of MSKCC.

Statistical methods

Data are presented as means ± SD or SEM as stated in the figure legends. Results were analyzed by unpaired Student's *t* test (two-tailed) or by ANOVA as stated in the text, and statistical significance was defined at $P < 0.05$. Pairwise multiple comparisons were performed using multiple *t* tests corrected for multiple comparisons with the Holm-Sidak method. All exact *P* values are provided. All statistical analyses were done with Prism software version 6.0 (GraphPad).

Supplementary Material

Refer to Web version on PubMed Central for supplementary material.

Acknowledgments

We thank G. Gunset for excellent technical assistance and R. Josowitz for excellent technical assistance, discussion, and manuscript editing. We thank K. Manova, S. Fujisawa, and Y. Romin for consulting and technical assistance for the microscopy studies, and J. Hendrikx for MoFlo cell sorts.

Funding: This work was supported by the Majors Family Foundation, the Mallah Fund, the Lake Road Foundation, the Mr. and Ms. Goodwyn Commonwealth Fund, and the Experimental Therapeutics Center at MSKCC. V.D.F. was supported by a training grant from the National Heart, Lung, and Blood Institute (T32 GM007739-31S1) to the Weill Cornell/Rockefeller/Sloan Kettering Tri-Institutional MD-PhD program. M.T. was supported by the Sloan-Kettering Institute Clinical Scholars Biomedical Research Training Program with funds granted by the Charles A. Dana Foundation.

REFERENCES AND NOTES

1. Blattman JN, Greenberg PD. Cancer immunotherapy: A treatment for the masses. Science. 2004; 305:200–205. [PubMed: 15247469]
2. Restifo NP, Dudley ME, Rosenberg SA. Adoptive immunotherapy for cancer: Harnessing the T cell response. Nat Rev Immunol. 2012; 12:269–281. [PubMed: 22437939]
3. Sadelain M, Brentjens R, Rivière I. The promise and potential pitfalls of chimeric antigen receptors. Curr Opin Immunol. 2009; 21:215–223. [PubMed: 19327974]
4. Turtle CJ, Hudecek M, Jensen MC, Riddell SR. Engineered T cells for anti-cancer therapy. Curr Opin Immunol. 2012; 24:633–639. [PubMed: 22818942]
5. Blazar BR, Murphy WJ, Abedi M. Advances in graft-versus-host disease biology and therapy. Nat Rev Immunol. 2012; 12:443–458. [PubMed: 22576252]
6. Brusko TM, Putnam AL, Bluestone JA. Human regulatory T cells: Role in autoimmune disease and therapeutic opportunities. Immunol Rev. 2008; 223:371–390. [PubMed: 18613848]
7. Kalos M, Levine BL, Porter DL, Katz S, Grupp SA, Bagg A, June CH. T cells with chimeric antigen receptors have potent antitumor effects and can establish memory in patients with advanced leukemia. Sci Transl Med. 2011; 3:95ra73.
8. Brentjens RJ, Rivière I, Park JH, Davila ML, Wang X, Stefanski J, Taylor C, Yeh R, Bartido S, Borquez-Ojeda O, Olszewska M, Bernal Y, Pegram H, Przybylowski M, Hollyman D, Usachenko Y, Pirraglia D, Hosey J, Santos E, Halton E, Maslak P, Scheinberg D, Jurcic J, Heaney M, Heller G, Frattini M, Sadelain M. Safety and persistence of adoptively transferred autologous CD19-targeted T cells in patients with relapsed or chemotherapy refractory B-cell leukemias. Blood. 2011; 118:4817–4828. [PubMed: 21849486]
9. Brentjens RJ, Davila ML, Riviere I, Park J, Wang X, Cowell LG, Bartido S, Stefanski J, Taylor C, Olszewska M, Borquez-Ojeda O, Qu J, Wasielewska T, He Q, Bernal Y, Rijo IV, Hedvat C, Kobos R, Curran K, Steinherz P, Jurcic J, Rosenblat T, Maslak P, Frattini M, Sadelain M. CD19-targeted T cells rapidly induce molecular remissions in adults with chemotherapy-refractory acute lymphoblastic leukemia. Sci Transl Med. 2013; 5:177ra38.
10. Morgan RA, Yang JC, Kitano M, Dudley ME, Laurencot CM, Rosenberg SA. Case report of a serious adverse event following the administration of T cells transduced with a chimeric antigen receptor recognizing *ERBB2*. Mol Ther. 2010; 18:843–851. [PubMed: 20179677]
11. Morgan RA, Chinnasamy N, Abate-Daga D, Gros A, Robbins PF, Zheng Z, Dudley ME, Feldman SA, Yang JC, Sherry RM, Phan GQ, Hughes MS, Kammula US, Miller AD, Hessman CJ, Stewart AA, Restifo NP, Quezado MM, Alimchandani M, Rosenberg AZ, Nath A, Wang T, Bielekova B, Wuest SC, Akula N, McMahon FJ, Wilde S, Mosetter B, Schendel DJ, Laurencot CM, Rosenberg SA. Cancer regression and neurological toxicity following anti-MAGE-A3 TCR gene therapy. J Immunother. 2013; 36:133–151. [PubMed: 23377668]
12. Cameron BJ, Gerry AB, Dukes J, Harper JV, Kannan V, Bianchi FC, Grand F, Brewer JE, Gupta M, Plesa G, Bossi G, Vuidepot A, Powlesland AS, Legg A, Adams KJ, Bennett AD, Pumphrey NJ, Williams DD, Binder-Scholl G, Kulikovskaya I, Levine BL, Riley JL, Varela-Rohena A, Stadtmauer EA, Rapoport AP, Linette GP, June CH, Hassan NJ, Kalos M, Jakobsen BK. Identification of a Titin-derived HLA-A1–presented peptide as a cross-reactive target for engineered MAGE A3–directed T cells. Sci Transl Med. 2013; 5:197ra103.
13. Linette GP, Stadtmauer EA, Maus MV, Rapoport AP, Levine BL, Emery L, Litzky L, Bagg A, Carreno BM, Cimino PJ, Binder-Scholl GK, Smethurst DP, Gerry AB, Pumphrey NJ, Bennett AD, Brewer JE, Dukes J, Harper J, Tayton-Martin HK, Jakobsen BK, Hassan NJ, Kalos M, June CH. Cardiovascular toxicity and titin cross-reactivity of affinity-enhanced T cells in myeloma and melanoma. Blood. 2013; 122:863–871. [PubMed: 23770775]
14. Ferrara JL, Levine JE, Reddy P, Holler E. Graft-versus-host disease. Lancet. 2009; 373:1550–1561. [PubMed: 19282026]
15. Kotsiou E, Davies JK. New ways to separate graft-versus-host disease and graft-versus-tumour effects after allogeneic haematopoietic stem cell transplantation. Br J Haematol. 2013; 160:133–145. [PubMed: 23121307]

16. Akpek G, Lee SM, Anders V, Vogelsang GB. A high-dose pulse steroid regimen for controlling active chronic graft-versus-host disease. Biol Blood Marrow Transplant. 2001; 7:495–502. [PubMed: 11669216]

17. Lupo-Stanghellini MT, Provasi E, Bondanza A, Ciceri F, Bordignon C, Bonini C. Clinical impact of suicide gene therapy in allogeneic hematopoietic stem cell transplantation. Hum Gene Ther. 2010; 21:241–250. [PubMed: 20121594]

18. Di Stasi A, Tey SK, Dotti G, Fujita Y, Kennedy-Nasser A, Martinez C, Straathof K, Liu E, Durett AG, Grilley B, Liu H, Cruz CR, Savoldo B, Gee AP, Schindler J, Krance RA, Heslop HE, Spencer DM, Rooney CM, Brenner MK. Inducible apoptosis as a safety switch for adoptive cell therapy. N Engl J Med. 2011; 365:1673–1683. [PubMed: 22047558]

19. Vogler I, Newrzela S, Hartmann S, Schneider N, von Laer D, Koehl U, Grez M. An improved bicistronic CD20/tCD34 vector for efficient purification and in vivo depletion of gene-modified T cells for adoptive immunotherapy. Mol Ther. 2010; 18:1330–1338. [PubMed: 20461062]

20. Kieback E, Charo J, Sommermeyer D, Blankenstein T, Uckert W. A safeguard eliminates T cell receptor gene-modified autoreactive T cells after adoptive transfer. Proc Natl Acad Sci USA. 2008; 105:623–628. [PubMed: 18182487]

21. Pardoll DM. The blockade of immune checkpoints in cancer immunotherapy. Nat Rev Cancer. 2012; 12:252–264. [PubMed: 22437870]

22. Sharma P, Wagner K, Wolchok JD, Allison JP. Novel cancer immunotherapy agents with survival benefit: Recent successes and next steps. Nat Rev Cancer. 2011; 11:805–812. [PubMed: 22020206]

23. Tivol EA, Borriello F, Schweitzer AN, Lynch WP, Bluestone JA, Sharpe AH. Loss of CTLA-4 leads to massive lymphoproliferation and fatal multiorgan tissue destruction, revealing a critical negative regulatory role of CTLA-4. Immunity. 1995; 3:541–547. [PubMed: 7584144]

24. Nishimura H, Nose M, Hiai H, Minato N, Honjo T. Development of lupus-like autoimmune diseases by disruption of the *PD-1* gene encoding an ITIM motif-carrying immunoreceptor. Immunity. 1999; 11:141–151. [PubMed: 10485649]

25. Wang J, Yoshida T, Nakaki F, Hiai H, Okazaki T, Honjo T. Establishment of NOD-*Pdcd1*$^{-/-}$ mice as an efficient animal model of type I diabetes. Proc Natl Acad Sci USA. 2005; 102:11823–11828. [PubMed: 16087865]

26. Parry RV, Chemnitz JM, Frauwirth KA, Lanfranco AR, Braunstein I, Kobayashi SV, Linsley PS, Thompson CB, Riley JL. CTLA-4 and PD-1 receptors inhibit T-cell activation by distinct mechanisms. Mol Cell Biol. 2005; 25:9543–9553. [PubMed: 16227604]

27. Topalian SL, Hodi FS, Brahmer JR, Gettinger SN, Smith DC, McDermott DF, Powderly JD, Carvajal RD, Sosman JA, Atkins MB, Leming PD, Spigel DR, Antonia SJ, Horn L, Drake CG, Pardoll DM, Chen L, Sharfman WH, Anders RA, Taube JM, McMiller TL, Xu H, Korman AJ, Jure-Kunkel M, Agrawal S, McDonald D, Kollia GD, Gupta A, Wigginton JM, Sznol M. Safety, activity, and immune correlates of anti–PD-1 antibody in cancer. N Engl J Med. 2012; 366:2443–2454. [PubMed: 22658127]

28. Hodi FS, O'Day SJ, McDermott DF, Weber RW, Sosman JA, Haanen JB, Gonzalez R, Robert C, Schadendorf D, Hassel JC, Akerley W, van den Eertwegh AJ, Lutzky J, Lorigan P, Vaubel JM, Linette GP, Hogg D, Ottensmeier CH, Lebbé C, Peschel C, Quirt I, Clark JI, Wolchok JD, Weber JS, Tian J, Yellin MJ, Nichol GM, Hoos A, Urba WJ. Improved survival with ipilimumab in patients with metastatic melanoma. N Engl J Med. 2010; 363:711–723. [PubMed: 20525992]

29. Pedicord VA, Montalvo W, Leiner IM, Allison JP. Single dose of anti–CTLA-4 enhances CD8^{+} T-cell memory formation, function, and maintenance. Proc Natl Acad Sci USA. 2011; 108:266–271. [PubMed: 21173239]

30. Velu V, Titanji K, Zhu B, Husain S, Pladevega A, Lai L, Vanderford TH, Chennareddi L, Silvestri G, Freeman GJ, Ahmed R, Amara RR. Enhancing SIV-specific immunity in vivo by PD-1 blockade. Nature. 2009; 458:206–210. [PubMed: 19078956]

31. Gade TP, Hassen W, Santos E, Gunset G, Saudemont A, Gong MC, Brentjens R, Zhong XS, Stephan M, Stefanski J, Lyddane C, Osborne JR, Buchanan IM, Hall SJ, Heston WD, Rivière I, Larson SM, Koutcher JA, Sadelain M. Targeted elimination of prostate cancer by genetically directed human T lymphocytes. Cancer Res. 2005; 65:9080–9088. [PubMed: 16204083]

32. Sadelain M, Brentjens R, Rivière I. The basic principles of chimeric antigen receptor design. Cancer Discov. 2013; 3:388–398. [PubMed: 23550147]
33. Kinoshita Y, Kuratsukuri K, Landas S, Imaida K, Rovito PM Jr, Wang CY, Haas GP. Expression of prostate-specific membrane antigen in normal and malignant human tissues. World J Surg. 2006; 30:628–636. [PubMed: 16555021]
34. Maher J, Brentjens RJ, Gunset G, Rivière I, Sadelain M. Human T-lymphocyte cytotoxicity and proliferation directed by a single chimeric TCRζ/CD28 receptor. Nat Biotechnol. 2002; 20:70–75. [PubMed: 11753365]
35. Teft WA, Kirchhof MG, Madrenas J. A molecular perspective of CTLA-4 function. Annu Rev Immunol. 2006; 24:65–97. [PubMed: 16551244]
36. Fu X, Tao L, Rivera A, Williamson S, Song XT, Ahmed N, Zhang X. A simple and sensitive method for measuring tumor-specific T cell cytotoxicity. PLOS One. 2010; 5:e11867. [PubMed: 20686618]
37. Brentjens RJ, Santos E, Nikhamin Y, Yeh R, Matsushita M, La Perle K, Quintás-Cardama A, Larson SM, Sadelain M. Genetically targeted T cells eradicate systemic acute lymphoblastic leukemia xenografts. Clin Cancer Res. 2007; 13:5426–5435. [PubMed: 17855649]
38. Markley JC, Sadelain M. IL-7 and IL-21 are superior to IL-2 and IL-15 in promoting human T cell–mediated rejection of systemic lymphoma in immunodeficient mice. Blood. 2010; 115:3508–3519. [PubMed: 20190192]
39. Chemnitz JM, Parry RV, Nichols KE, June CH, Riley JL. SHP-1 and SHP-2 associate with immunoreceptor tyrosine-based switch motif of programmed death 1 upon primary human T cell stimulation, but only receptor ligation prevents T cell activation. J Immunol. 2004; 173:945–954. [PubMed: 15240681]
40. Yokosuka T, Takamatsu M, Kobayashi-Imanishi W, Hashimoto-Tane A, Azuma M, Saito T. Programmed cell death 1 forms negative costimulatory microclusters that directly inhibit T cell receptor signaling by recruiting phosphatase SHP2. J Exp Med. 2012; 209:1201–1217. [PubMed: 22641383]
41. Bryceson YT, Long EO. Line of attack: NK cell specificity and integration of signals. Curr Opin Immunol. 2008; 20:344–352. [PubMed: 18439809]
42. Amarnath S, Mangus CW, Wang JC, Wei F, He A, Kapoor V, Foley JE, Massey PR, Felizardo TC, Riley JL, Levine BL, June CH, Medin JA, Fowler DH. The PDL1-PD1 axis converts human T_H1 cells into regulatory T cells. Sci Transl Med. 2011; 3:111ra120.
43. Peggs KS, Quezada SA, Allison JP. Cell intrinsic mechanisms of T-cell inhibition and application to cancer therapy. Immunol Rev. 2008; 224:141–165. [PubMed: 18759925]
44. Rudd CE. The reverse stop-signal model for CTLA4 function. Nat Rev Immunol. 2008; 8:153–160. [PubMed: 18219311]
45. Uhlen M, Oksvold P, Fagerberg L, Lundberg E, Jonasson K, Forsberg M, Zwahlen M, Kampf C, Wester K, Hober S, Wernerus H, Björling L, Ponten F. Towards a knowledge-based Human Protein Atlas. Nat Biotechnol. 2010; 28:1248–1250. [PubMed: 21139605]
46. Campoli M, Ferrone S. HLA antigen changes in malignant cells: Epigenetic mechanisms and biologic significance. Oncogene. 2008; 27:5869–5885. [PubMed: 18836468]
47. Cui Y, Ying Y, van Hasselt A, Ng KM, Yu J, Zhang Q, Jin J, Liu D, Rhim JS, Rha SY, Loyo M, Chan AT, Srivastava G, Tsao GS, Sellar GC, Sung JJ, Sidransky D, Tao Q. *OPCML* is a broad tumor suppressor for multiple carcinomas and lymphomas with frequently epigenetic inactivation. PLOS One. 2008; 3:e2990. [PubMed: 18714356]
48. Singh K, Mogare D, Giridharagopalan RO, Gogiraju R, Pande G, Chattopadhyay S. p53 target gene SMAR1 is dysregulated in breast cancer: Its role in cancer cell migration and invasion. PLOS One. 2007; 2:e660. [PubMed: 17668048]
49. Meimei L, Peiling L, Baoxin L, Changmin L, Rujin Z, Chunjie H. Lost expression of *DCC* gene in ovarian cancer and its inhibition in ovarian cancer cells. Med Oncol. 2011; 28:282–289. [PubMed: 20054719]
50. Tsuboi S, Hatakeyama S, Ohyama C, Fukuda M. Two opposing roles of *O*-glycans in tumor metastasis. Trends Mol Med. 2012; 18:224–232. [PubMed: 22425488]

51. Tsuchiya B, Sato Y, Kameya T, Okayasu I, Mukai K. Differential expression of N-cadherin and E-cadherin in normal human tissues. Arch Histol Cytol. 2006; 69:135–145. [PubMed: 16819153]
52. Chaffer CL, Weinberg RA. A perspective on cancer cell metastasis. Science. 2011; 331:1559–1564. [PubMed: 21436443]
53. Stephan MT, Ponomarev V, Brentjens RJ, Chang AH, Dobrenkov KV, Heller G, Sadelain M. T cell–encoded CD80 and 4-1BBL induce auto- and transcostimulation, resulting in potent tumor rejection. Nat Med. 2007; 13:1440–1449. [PubMed: 18026115]
54. Burshtyn DN, Davidson C. Natural killer cell conjugate assay using two-color flow cytometry. Methods Mol Biol. 2010; 612:89–96. [PubMed: 20033636]
55. Themeli M, Kloss CC, Ciriello G, Fedorov VD, Perna F, Gonen M, Sadelain M. Generation of tumor-targeted human T lymphocytes from induced pluripotent stem cells for cancer therapy. Nat Biotechnol. 2013; 31:928–933. [PubMed: 23934177]
56. Yuan J, Latouche JB, Reagan JL, Heller G, Riviere I, Sadelain M, Young JW. Langerhans cells derived from genetically modified human $CD34^+$ hemopoietic progenitors are more potent than peptide-pulsed Langerhans cells for inducing antigen-specific $CD8^+$ cytolytic T lymphocyte responses. J Immunol. 2005; 174:758–766. [PubMed: 15634896]

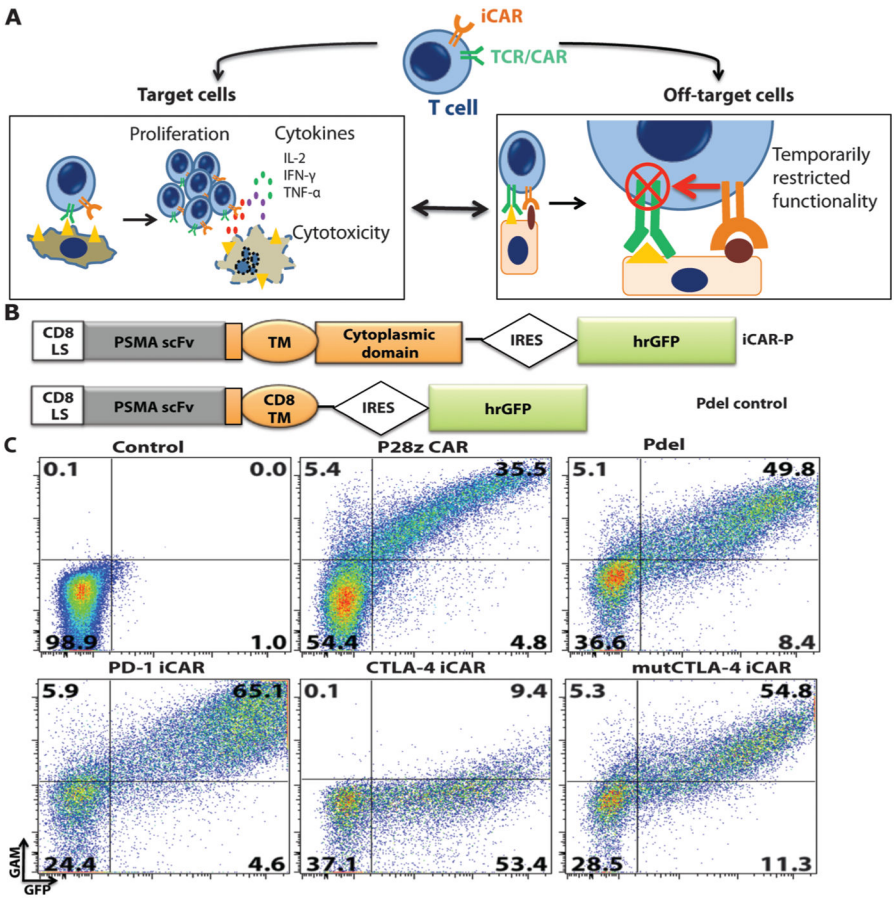

Fig. 1. iCAR strategy, design, and expression in primary human T cells

(**A**) T cells with specificity for both tumor and off-target tissues can be restricted to tumor only by using an antigen-specific iCAR introduced into the T cells to protect the off-target tissue. (**B**) Schematic diagram of the bicistronic vectors used for iCARs and Pdel. iCAR-P: a spacer, transmembrane, and intracellular tail of each inhibitory receptor were cloned into a previously described retroviral vector having a CD8 leader sequence (LS). IRES, internal ribosomal entry site; hrGFP, humanized *Renilla* green fluorescent protein reporter. A Pdel control vector was designed with a spacer and CD8 transmembrane (TM) domain, and lacking an intracellular tail. (**C**) Cell surface expression of the iCARs was assessed by flow cytometry in transduced primary human T cells. Dot plots are representative of eight different donors. GAM, goat anti-mouse immunoglobulin G $F(ab')_2$ antibody that binds to the murine-derived extracellular domain of the CAR.

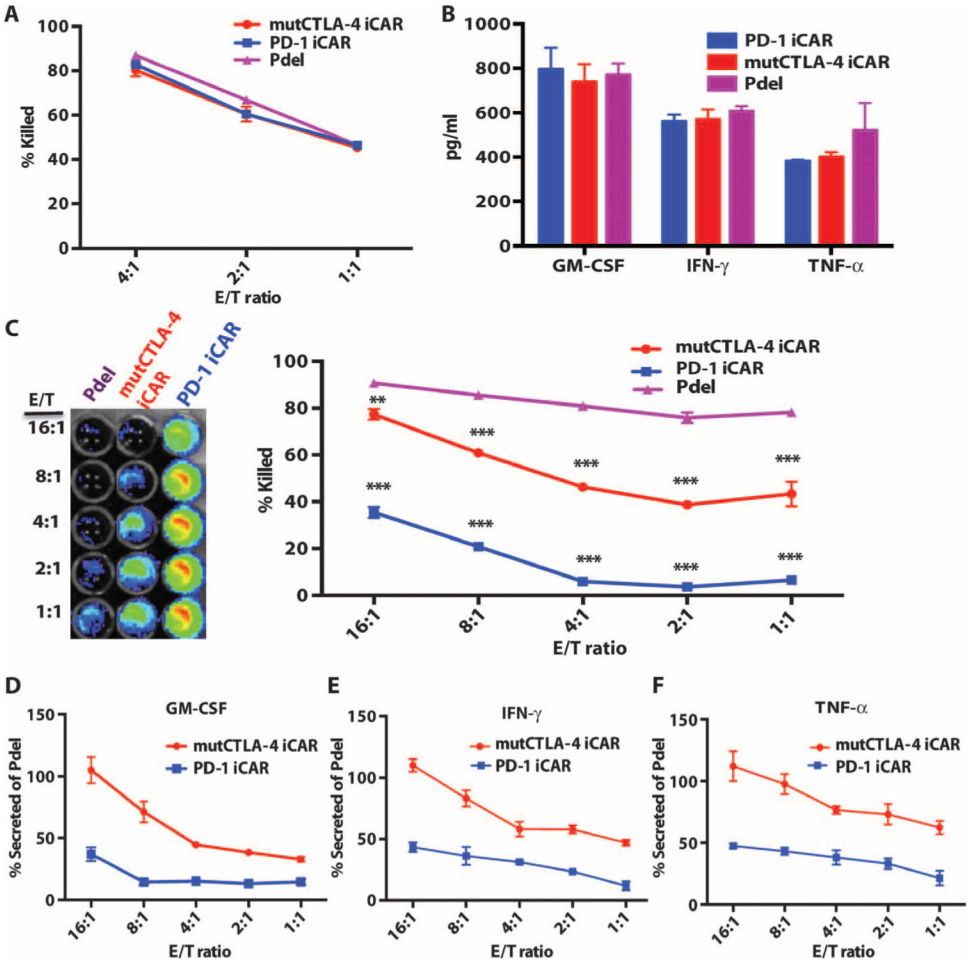

Fig. 2. iCARs protect iPS-fib from TCR-mediated allogeneic reactions

Control Pdel- or iCAR-transduced T cells primed with allogeneic moDCs were incubated with iPS-derived fibroblasts (iPS-fib) expressing click beetle luciferase (CBL), isogenic to the moDCs, using a range of E/T ratios. (**A**) Pdel-, PD-1–, or mutCTLA-4 iCAR-P–transduced T cells reacting against target iPS-fib ($n = 3$ per condition). Killing of the iPS-fib was quantified with the Bright-Glo assay system. (**B**) Cytokine secretion in cell culture supernatants from (A) at 4:1 E/T ratio was assessed at 18 hours. GM-CSF, granulocyte-macrophage colony-stimulating factor; IFN-γ, interferon-γ; TNF-α, tumor necrosis factor-α. (**C**) Pdel- or iCAR-positive T cells were incubated for 24 hours with off-target iPS-fib expressing PSMA (iPS-fib-PSMA), and luciferase signal (left) was quantified (right) ($n = 3$ for each condition). (**D** to **F**) Cytokine secretion measured at 24 hours in cell culture supernatants from (C). Error bars represent ±SEM. *$P < 0.01$, ***$P < 0.001$ by analysis of variance (ANOVA) comparing iCARs to Pdel and post hoc analysis with multiple *t* tests corrected with the Holm-Sidak method. Raw data and *P* values are provided in the Supplementary Materials.

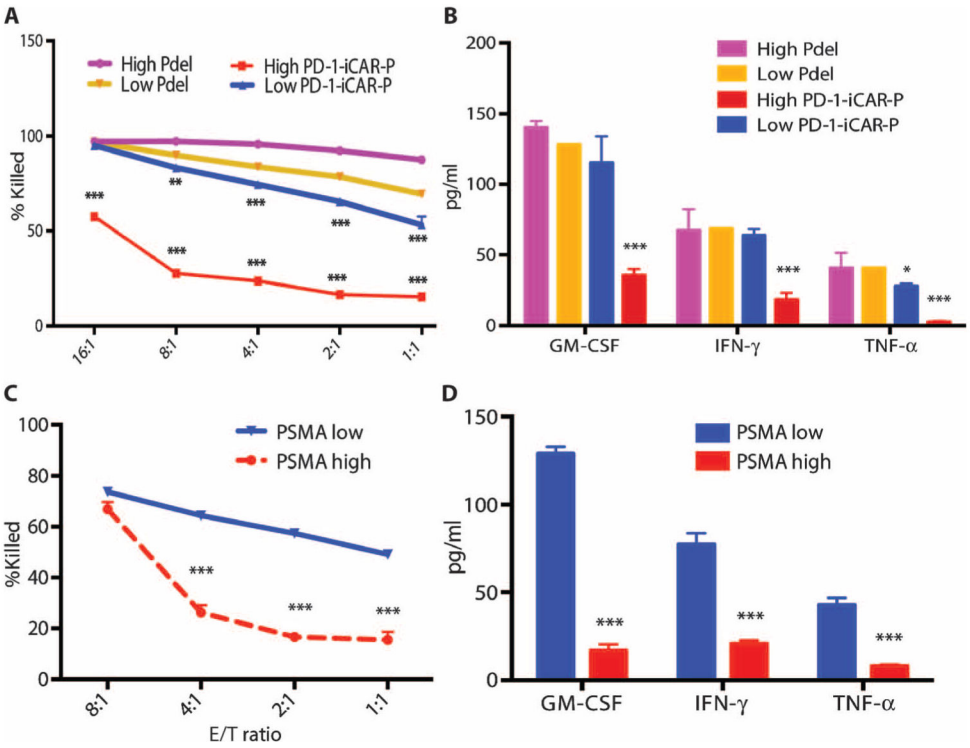

Fig. 3. iCARs function in a stoichiometric manner

(**A**) Pdel- or PD-1 iCAR-P–transduced alloreactive T cells were sorted for high or low expression of each respective receptor, as shown in fig. S5A, and were seeded on iPS-fib-PSMA–expressing CBL. Killing of iPS-fib-PSMA relative to untreated cells was assessed with the Bright-Glo assay system (n = 3 for each condition). (**B**) Cytokine secretion, measured at 24 hours in the cell culture supernatant from (A) at 4:1 E/T ratio. (**C**) PD-1 iCAR-P–transduced alloreactive T cells were incubated with iPS-fib-PSMA sorted for high or low levels of PSMA expression as shown in fig. S5B. Killing of each population relative to untreated cells was quantified with the Bright-Glo assay system (n = 3 per condition). **D**) Cytokines from (C) were assessed at 24 hours. Error bars represent ±SEM. ***P < 0.001 by Student's t test. Error bars represent ±SEM. *P < 0.01, ***P < 0.001 by ANOVA comparing to high Pdel group and post hoc analysis with multiple t tests corrected with the Holm-Sidak method. Raw data and P values are provided in the Supplementary Materials.

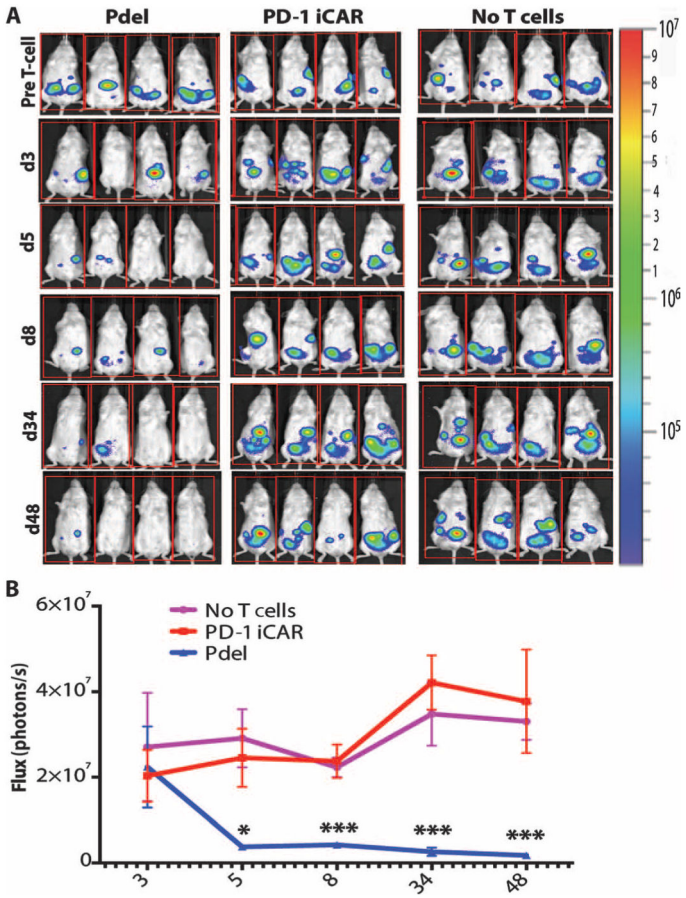

Fig. 4. iCARs limit allogeneic responses in vivo

NOD/SCID/γ_c^- mice were injected intraperitoneally with 1×10^6 iPS-derived fibroblasts expressing CBL/PSMA (iPS-fib-PSMA) and, 7 days later, were treated intraperitoneally with 5×10^5 PD-1 iCAR-P– or Pdel-transduced, sorted, alloreactive T cells. Untreated mice (no T cells) were used as control. (**A**) Survival of iPS-fib-PSMA was assessed by BLI before and at selected time points after T cell infusion. Images of four representative mice from each group are shown. (**B**) Total body flux (photons per second) for each mouse was quantified and averaged per group ($n = 5$ per group). Error bars represent ±SEM. *$P < 0.05$, **$P < 0.01$ by ANOVA comparing to Pdel and post hoc analysis with multiple t tests corrected with the Holm-Sidak method. Raw data and P values are provided in the Supplementary Materials.

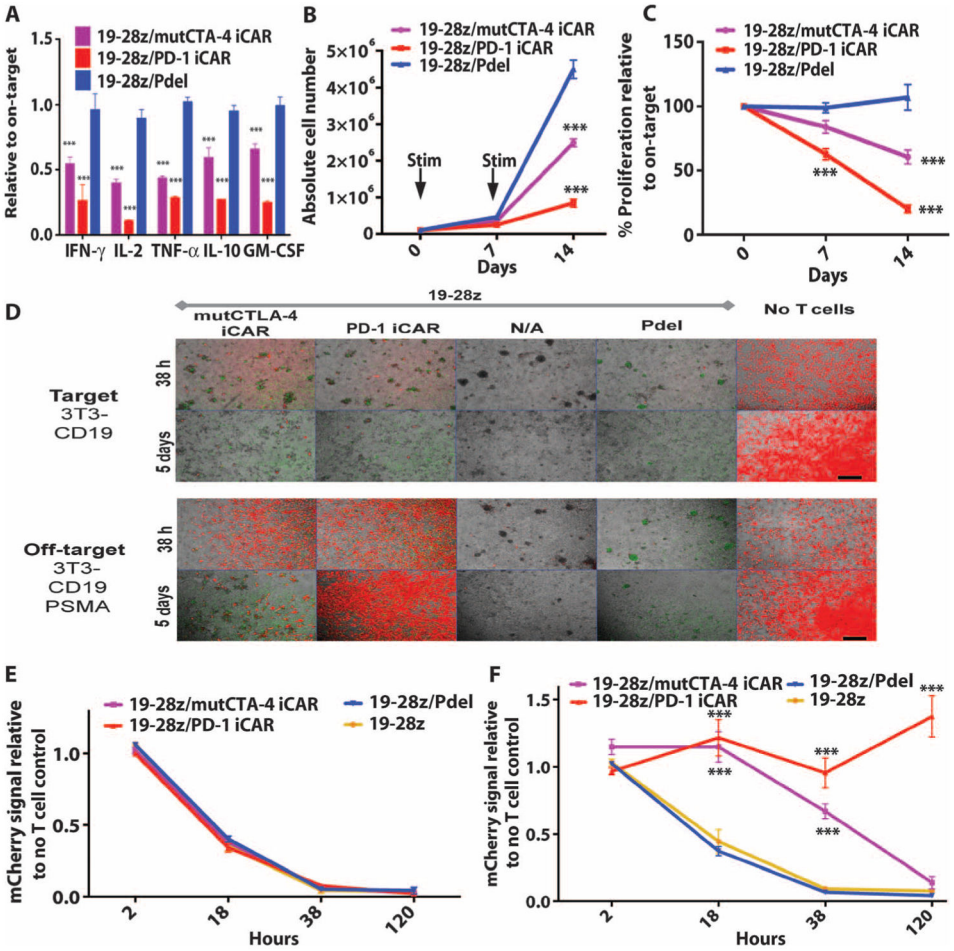

Fig. 5. iCARs inhibit human T cell cytokine release, proliferation, and target cell elimination driven by 19-28z CAR

(**A**) Luminex multiplex cytokine analysis of culture supernatant 24 hours after seeding dual-sorted 19-28z/Pdel– or 19-28z/iCAR–transduced human T cells on 3T3-CD19 (target) or 3T3-CD19-PSMA (off-target) AAPCs. The data are represented as a ratio of off-target/target values and pooled from three independent experiments ($n = 6$ wells per condition). Error bars represent ±SEM. $^{**}P < 0.01$, $^{***}P < 0.001$ by ANOVA comparing iCARs to Pdel and post hoc analysis with multiple *t* tests corrected with the Holm-Sidak method. (**B**) Absolute counts of 19-28z/Pdel or 19-28z/iCAR T cells stimulated on days 0 and 7 with off-target AAPCs. No exogenous cytokines were added. Data are representative of six independent experiments. (**C**) Proliferation of 19-28z/Pdel or 19-28z/iCAR T cells stimulated on days 0 and 7 with off-target AAPCs relative to proliferation on target AAPCs. No exogenous cytokines were added. Data are representative of six independent experiments. (**D**) T cells seeded at a 1:1 ratio on target and off-target mCherry^{+} AAPCs. Images at 38 hours and 5 days from one of five independent experiments are shown. Scale bars, 0.5 mm. (**E** and **F**) Quantification of mCherry signal from (D) against CD19 targets (E) or CD19-PSMA off-target cells (F), as described in Materials and Methods. Error bars represent ±SEM. $^{**}P < 0.01$, $^{***}P < 0.001$ by Student's *t* test. Raw data and *P* values are provided in the Supplementary Materials.

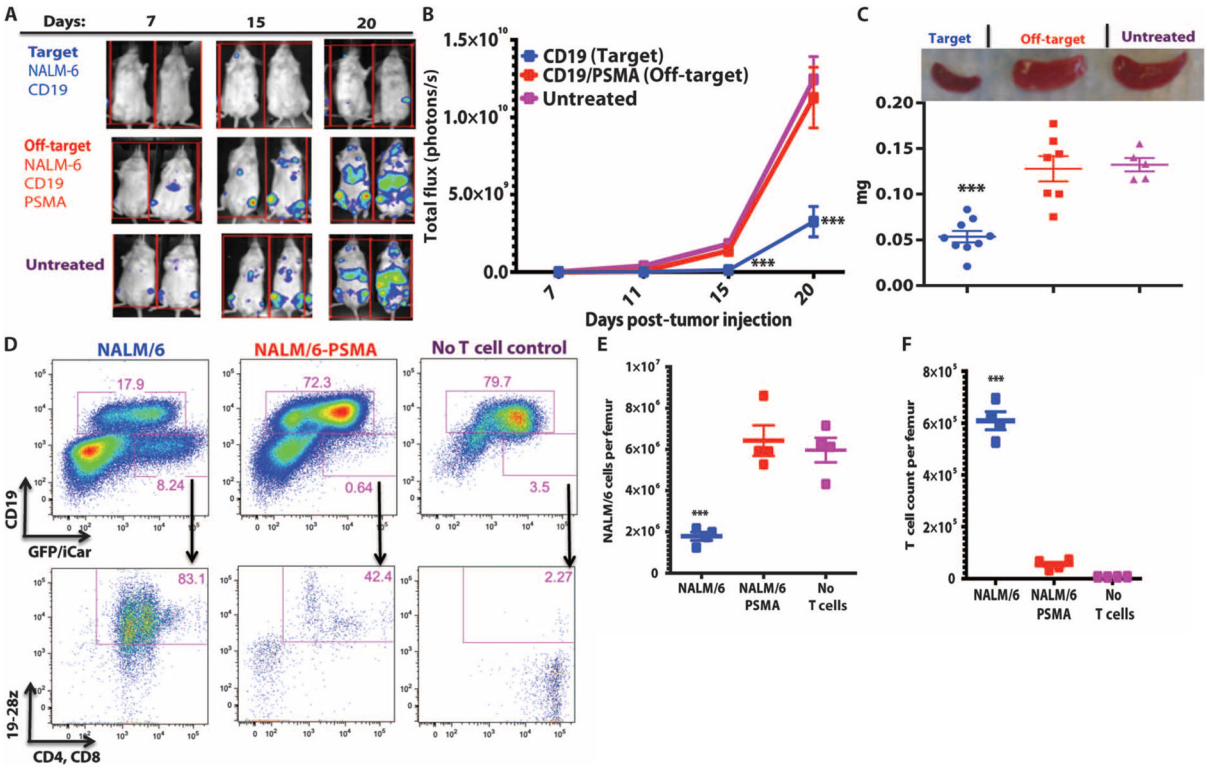

Fig. 6. iCARs restrict 19-28z CAR target cell specificity in vivo

(**A**) BLI depicting the tumor progress of NALM/6 or NALM/6-PSMA in NOD/SCID/γ_c^- mice treated with sorted 19-28z/PD-1 iCAR-P T cells. Untreated mice (no T cells) were used as control. (**B**) Tumor burden for each mouse was quantified, and average total flux per group is shown. (**C**) Spleen weight of mice from (A) sacrificed at day 21. Each dot represents one recipient mouse. (**D**) Flow cytometric analysis of the femur bone marrow from (C) for the presence of tumor cells ($CD19^+GFP^+$) and T cells ($CD19^-$19-28z/$GFP^+CD4^+CD8^+$). 19-28z expression was assessed by staining for LNGFR receptor whose complementary DNA (cDNA) is linked to 19-28z and is used as a detection marker. (**E** and **F**) Absolute numbers of tumor cells (E) and of $CD19^-$19-28z/$GFP^+CD4^+CD8^+$ T cells (F) in the spleens from (C) were quantified by flow cytometry with CountBright beads ($n = 4$). Error bars represent ±SEM. $^{**}P < 0.01$, $^{***}P < 0.001$ by Student's t test.

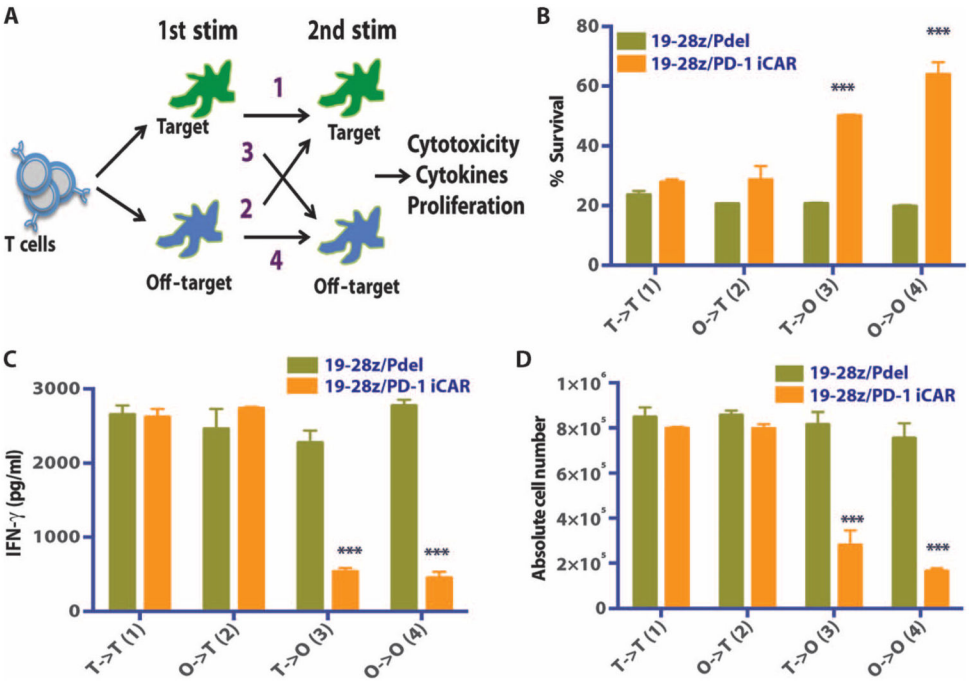

Fig. 7. iCAR function is temporary and reversible

(**A**) 19-28z/Pdel or 19-28z/PD-1 iCAR-P T cells were incubated with target (T) or off-target (O) AAPCs for the first stimulation. After 3 or 7 days, the cells from each group were restimulated with either target [T→T (1) or O→T (2)] or off-target [T→O (3) or O→O (4)] AAPCs in a crisscross manner to analyze the effects of the first stimulation on subsequent T cell function. (**B**) Killing of target (T) or off-target (O) AAPCs at 24 hours after incubation with each T cell group (second stimulation) was analyzed with the Bright-Glo assay system ($n = 3$ for each condition). (**C**) Secretion of effector cytokines in the cell culture supernatant from (B) was analyzed 24 hours after the second stimulation, and interferon-γ (IFN-γ) is shown as a representative result ($n = 3$ for each condition). (**D**) T cell proliferation at day 7 after the second stimulation ($n = 3$ for each condition). Error bars represent ±SEM. Statistical comparison was performed within each condition (that is, T→T Pdel versus PD-1 iCAR-P). ***$P < 0.001$ by Student's t test.

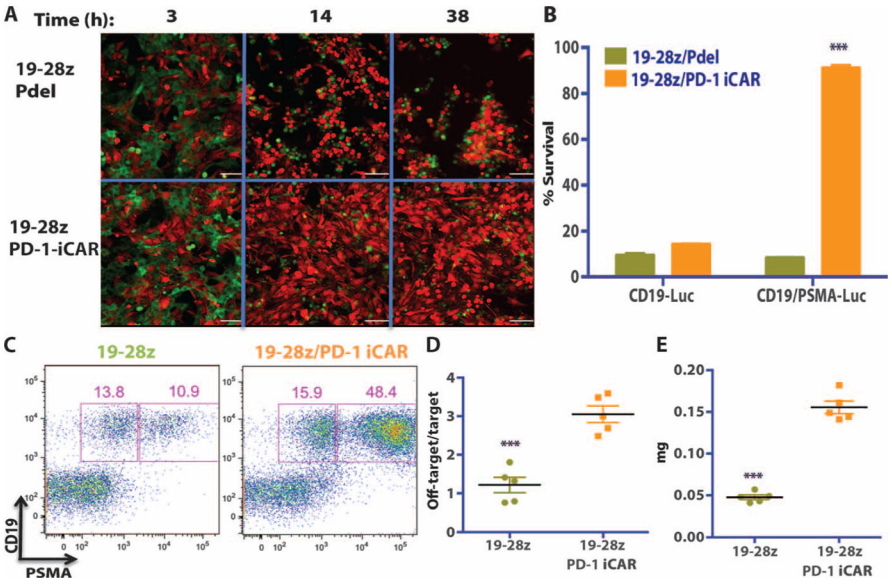

Fig. 8. iCAR- and CAR-expressing T cells discern targets in vitro and vivo

(**A**) 19-28z/Pdel or 19-28z/PD-1 iCAR-P T cells were incubated with a 1:1 mix of target ($CD19^+GFP^+$, green) and off-target ($CD19^+PSMA^+mCherry^+$, red) AAPCs, and time-lapse microscopy was used to visualize real-time killing of each population for 38 hours. Representative images are shown, and full-length movies are available in movie S1 (A and B). Scale bars, 0.1 mm. (**B**) As in (A), 19-28z/Pdel or 19-28z/PD-1 iCAR-P T cells were incubated with a 1:1 mix of target ($CD19^+$) and off-target ($CD19^+PSMA^+$) AAPCs. Killing of each AAPC population was assessed in parallel experiments where one of each AAPC type was labeled with CBL ($CD19^+CBL^+$/$CD19^+PSMA^+$ mix or $CD19^+$/$CD19^+PSMA^+CBL^+$ mix). Killing was quantified with the Bright-Glo assay system at 38 hours ($n = 3$ for each condition). (**C** to **E**) NOD/SCID/γ_c^- mice were injected with a 1:1 mixture of NALM/6 and NALM/6-PSMA cells and treated with 19-28z or 19-28z/PD-1 iCAR-P T cells. (C) Upon sacrifice, the presence of the target and off-target NALM/6 cells in the bone marrow was analyzed by flow cytometry. (D) Ratio of target/off-target NALM/6 cells in the bone marrow of sacrificed mice was quantified by flow cytometry. (E) Spleen weight of treated mice was also recorded at sacrifice. Error bars represent ±SEM. ***$P <$ 0.001 by Student's *t* test.